JOURNAL OF VIROLOGY, Mar. 2000, p. 2885–2887 Vol. 74, No. 6
0022-538X/00/$04.00+0

NOTES

The Intact Retroviral Env Glycoprotein of Human Foamy Virus Is a Trimer

THOMAS WILK,[1] FELIX DE HAAS,[1] ANDREA WAGNER,[2] TWAN RUTTEN,[1] STEPHEN FULLER,[1,3] ROLF M. FLÜGEL,[2] AND MARTIN LÖCHELT[2]*

Abteilung Retrovirale Genexpression, Forschungsschwerpunkt Angewandte Tumorvirologie, Deutsches Krebsforschungszentrum,[2] Structural Biology Programme, European Molecular Biology Laboratory, Heidelberg, Germany,[1] and Structural Biology Division, Wellcome Trust Centre for Human Genetics, University of Oxford, Oxford, United Kingdom[3]

Received 29 September 1999/Accepted 8 December 1999

Electron microscopy of negatively stained human foamy virus particles provides direct evidence for the trimeric nature of intact Env surface glycoproteins. Three-dimensional image reconstruction reveals that the Env trimer is a tapering spike 14 nm in length. The spikes were often arranged in hexagonal rings which shared adjacent Env trimers.

The structure and organization of the intact retrovirus envelope (Env) glycoprotein have remained a matter of dispute (5, 15). This protein complex, which plays a crucial role in the virus life cycle, comprises a transmembrane and a surface domain. The unprecedented clarity of electron micrographs of isolated human foamy virus (HFV) allowed direct visualization of the trimeric nature of the intact Env protein of this retrovirus (Fig. 1).

Electron microscopy (EM) of negatively stained (14) gradient-purified HFV particles derived from the supernatant of HFV-infected Hel299 cells (16) yielded striking surface images in which the threefold symmetry of Env protein complexes was apparent (Fig. 1). Frequently, the entire surface of the virion was covered with spikes clustered in six-membered rings. Axial views revealed three distinct subunits of the HFV Env trimer separated by 4.5 nm, as measured from the center of adjacent monomers in the trimeric assemblies (Fig. 1b, arrowheads). Monomeric HFV Env proteins were not detectable. The grouping of Env trimers into hexameric clusters generated centrally located, stain-filled holes of about 8 nm in diameter between the edges of opposing trimers in the six-membered rings (Fig. 1b, asterisks). Adjacent hexameric rings always shared two trimers. On those particles which carried clearly visible spikes, the hexameric arrangement was usually retained, while isolated Env trimers were almost absent on intact HFV particles.

The hexameric clustering was less stable than the trimer. We observed several cases in which staining had disrupted this arrangement so that the trimers were displaced. This dislocation did not disturb the internal arrangement of spike trimers, demonstrating the independence of the trimers and their intrinsic stability. The fact that all hexamers contained intact trimers demonstrates that the integrity of the trimeric complex is necessary for network formation on the surface of the virion.

* Corresponding author. Mailing address: Abteilung Retrovirale Genexpression, Forschungsschwerpunkt Angewandte Tumorvirologie, Deutsches Krebsforschungszentrum, Im Neuenheimer Feld 242, 69009 Heidelberg, Germany. Phone: 49-6221-424864. Fax: 49-6221-424865. E-mail: m.loechelt@dkfz-heidelberg.de.

Side views of Env complexes at the periphery of the particles revealed a spike length of 13.8 nm in agreement with previous reports (3, 8). The use of negative stain in this system had the advantage that it provided single-sided views of the structure. Cryo-EM produced similar images of the spikes (unpublished observations), but yielded a more complex image of the entire virion due to superposition.

The threefold nature of the axial views of the spike was tested by rotational correlation of the images. Analysis of 17 axial views showed that the highest peaks of rotational correlation averaged 119.4° (±8.99°), with a second peak at 241.2° (±9.60°), corresponding to multiples of 120° expected for threefold symmetry. No evidence of any other symmetry (e.g., two-, four-, five-, or sixfold) was observed in the rotational correlation analysis.

We took advantage of the one-sided nature of the negatively stained images to determine the three-dimensional structure of the HFV spike. Figures 2 and 3 show details of the reconstruction process. Images of individual trimers were taken to represent views of the same structure from a range of orientations. Identification of the relative orientations of these views allows the calculation of the three-dimensional structure which gave rise to them (9).

A model-based iterative approach (9) was used to reconstruct the density in a series of refinement cycles. The initial model was generated by combining axial and side views of closely packed spikes in which three neighbors were present. Threefold symmetry was then imposed along the trimer axis. This symmetrized model was then used to determine the relative orientations of 626 images by comparing them to the full range of projections for the calculation of a more reliable reconstruction. This process of model generation, imposition of axial threefold symmetry, and determination of improved orientations was repeated four times. The resulting three-dimensional structure is shown in Fig. 2I, J, K, and L, with the corresponding projections (E, F, G, and H) and averaged particle images (A, B, C, and D).

The improvement in the reconstruction during the cycles of refinement was monitored by Fourier shell correlation (FSC) (11) between two independent reconstructions generated from

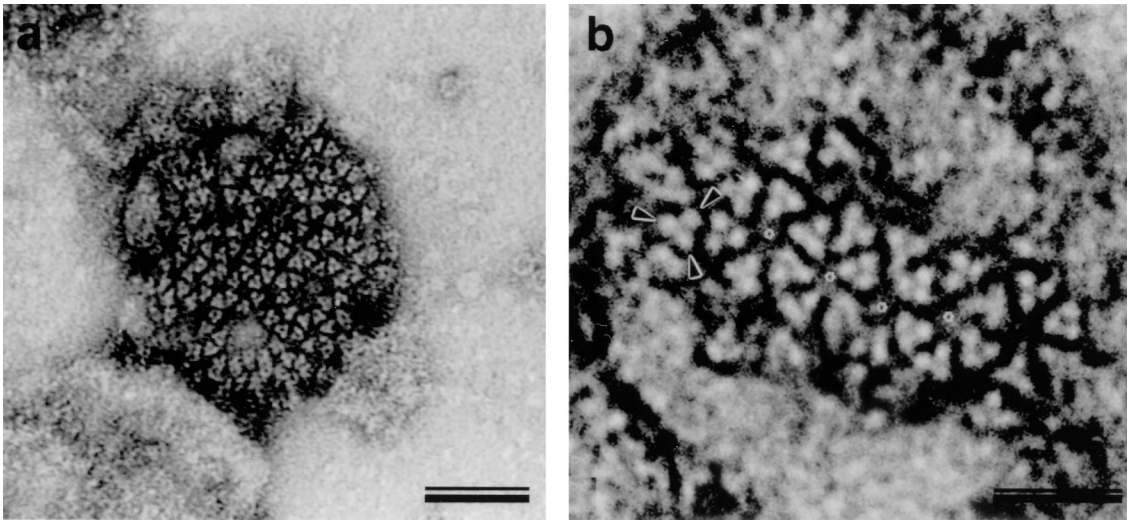

FIG. 1. Surface features of HFV particles detected by negative-staining EM. HFV isolated from the supernatant of infected Hel299 cells 4 days postinfection was purified by sucrose gradient centrifugation, and rapid, negative staining with uranyl acetate revealed surface features. Particles with a diameter of ~100 nm often showed a network of trimeric viral spike proteins on the particle surface and were predominantly arranged into rings of six subunits. When grouped in hexameric rings, a stain-filled hole with a diameter of about 8 nm was formed (b, asterisks). Adjacent rings always shared two completely integrated spikes. Images at higher magnification revealed three separate densities (arrowheads) in the triangular spike (b). Bars represent 50 nm (a) and 25 nm (b).

half-data sets (Fig. 3). The resolution at which the FSC value reached 0.5 serves as a measure of the reproducibility of the structure. Cycles of refinement caused this resolution to improve from its initial value of 3.6 nm to a final value of 3.4 nm in four cycles. The surface representations shown in Fig. 2 are low-pass filtered to this 3.4-nm resolution to remove details which are not preserved between the independent reconstructions.

The axial threefold symmetry of the density (Fig. 2) is imposed by the reconstruction process; however, the distribution of density within the threefold structure is determined by the density in the input images. The trimer in the center of the

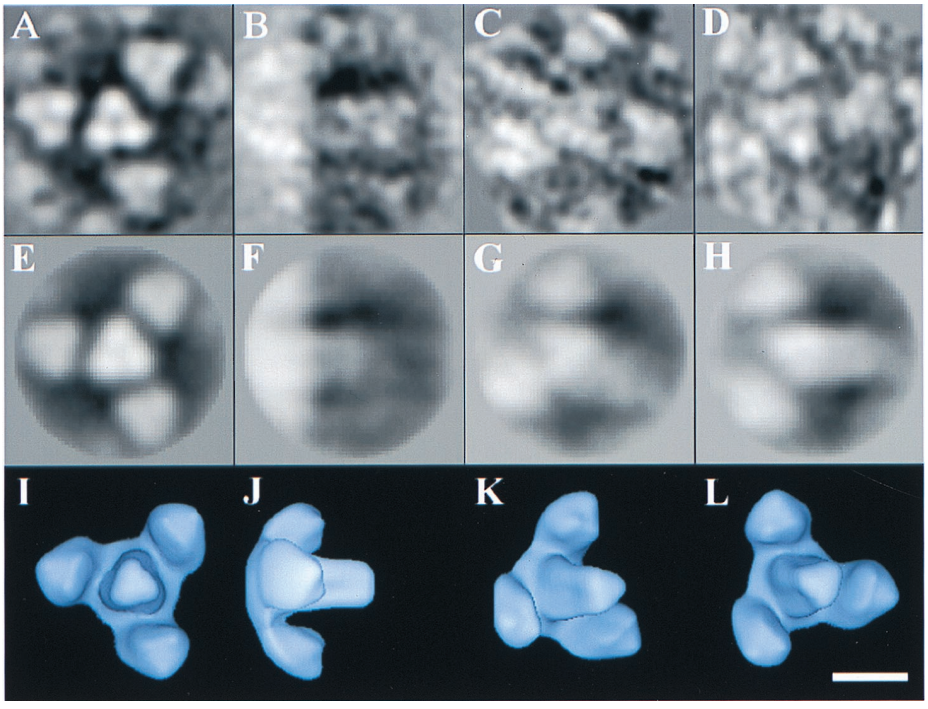

FIG. 2. Three-dimensional reconstruction of HFV spike glycoproteins. The reconstruction was performed with 626 images of negatively stained HFV Env trimers in hexagonal clusters by using a model-based, iterative approach. The top row of the figure shows the averaged particle images (A, B, C, and D) corresponding to the projections (E, F, G, and H) of the reconstruction shown in the middle row. The bottom row shows surface representations of the reconstruction (I, J, K, and L) contoured at a volume which corresponds to that expected for four Env trimers. The four views displayed are at the following orientations of θ, φ: 0°, 0° (A, E, and I), 90°, 0° (B, F, and J), 45°, 30° (C, G, and K), and 30°, 180° (D, H, and L), where the z axis (θ, φ = 0°, 0°) lies along the threefold axis. The bar represents 10 nm.

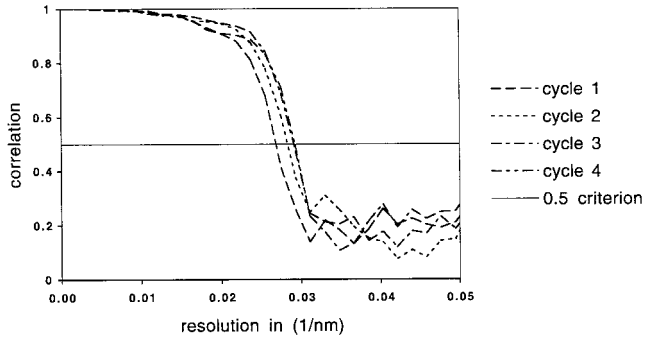

FIG. 3. Improvement of the image reconstruction with iterated cycles of refinement. The 626 particle images were divided into two sets and used to generate independent reconstructions. Comparison of these two reconstructions by FSC defined the resolution of the reproducible detail between the reconstructions. The resolution improved from 3.6 nm in the first cycle through 3.4 nm in the fourth cycle, as seen by the shift in the position at which the FSC curve first drops to a value of 0.5 (11).

reconstruction is clearer than the surrounding three trimers. We believe this reflects variation in the curvature of the virion surface, but it could also reflect variable spacing between trimers in the hexameric cluster or variation in the staining of individual trimers.

Our reconstruction reveals the HFV Env complexes as trimeric, tapering spikes with a depression at the tip and a volume consistent with that expected for a trimeric complex of single Env subunits (Fig. 2, bottom row). The reconstructed images of HFV Env explain the spiky appearance of foamy viruses seen in conventional EM. They contrast with the knob-like models of the retrovirus spike deduced from images of human immunodeficiency virus type 1 (3, 8).

Certain features of the molecular biology of foamy viruses (e.g., the requirement of Env for particle budding) are peculiar to this group of retroviruses (2, 6, 7, 10). We expect, however, that the trimeric nature of the HFV Env complexes is a common feature of retrovirus spikes. This inference is supported by structural and crystallographic data obtained from recombinant retroviral Env subdomains and EM studies that show a triangular shape for lentivirus spike proteins (4, 13, 15). Foamy virus Env proteins display structural homology to other retrovirus Env proteins (12). The fact that the trimeric nature of the HFV spike is more apparent than in other retroviruses may reflect greater stability of foamy virus Env assemblies.

Surface glycoproteins play a crucial role in the life cycle of enveloped viruses, both allowing entry into the host cell and being of prime importance for elimination and clearance of the virus by host defense mechanisms (1, 5, 15). A deeper understanding of their structure and conformation thus has important implications for biomedical applications, especially for persisting viruses which are not eliminated by the host (1, 15). The structures of Env-derived subdomains from human immunodeficiency virus and other retroviruses obtained by nuclear magnetic resonance and X-ray crystallography represent the conformation of the protein after activation for fusion. In contrast, our observations show the value of the foamy virus system for depicting the structure and function of the native retrovirus Env protein complex before the activation for fusion has occurred.

We thank Jennifer Reed for critical reading of the manuscript and Harald zur Hausen for continuous support.

This work was supported by Deutsche Forschungsgemeinschaft grant LO 700/1-2 to M. Löchelt. T. Wilk was supported by Deutsche Forschungsgemeinschaft grant FU354/1-1, T. Rutten was supported by a Human Frontiers Science Foundation grant (RG 102), and F. de Haas was supported by a European Union Biotechnology grant (BIO4-CT97-2364) to S. Fuller.

REFERENCES

1. **Fass, D., and P. S. Kim.** 1995. Dissection of a retrovirus envelope protein reveals structural similarity to influenza hemagglutinin. Curr. Biol. **5:**1377–1383.
2. **Fischer, N., M. Heinkelein, D. Lindemann, J. Enssle, C. Baum, E. Werder, H. Zentgraf, J. G. Müller, and A. Rethwilm.** 1999. Foamy virus particle formation. J. Virol. **72:**1610–1615.
3. **Gelderblom, H., and H. Frank.** 1987. Spumavirinae, p. 305–311. *In* M. V. Nermut and A. C. Steven (ed.), Animal virus structure. Elsevier Science Publishers, Amsterdam, The Netherlands.
4. **Grief, C., D. J. Hockley, C. E. Fromholc, and P. A. Kitchin.** 1999. The morphology of simian immunodeficiency virus as shown by negative staining electron microscopy. J. Gen. Virol. **70:**2215–2219.
5. **Hunter, E.** 1997. Viral entry and receptors, p. 71–120. *In* J. M. Coffin, S. Hughes, and H. E. Varmus (ed.), Retroviruses. Cold Spring Harbor Laboratory Press, Cold Spring Harbor, N.Y.
6. **Linial, M. L.** 1999. Foamy viruses are unconventional retroviruses. J. Virol. **73:**1747–1755.
7. **Löchelt, M., and R. M. Flügel.** 1995. The molecular biology of primate spumaviruses, p. 239–292. *In* J. A. Levy (ed.), The retroviridae, vol. 4. Plenum Press, New York, N.Y.
8. **Nermut, M. V., and D. J. Hockley.** 1996. Comparative morphology and structural classification of retroviruses. Curr. Top. Microbiol. Immunol. **214:** 1–24.
9. **Penczek, P., M. Radermacher, and J. Frank.** 1992. Three-dimensional reconstruction of single particles embedded in ice. Ultramicroscopy **40:**33–53.
10. **Rethwilm, A.** 1995. Regulation of foamy virus gene expression. Curr. Top. Microbiol. Immunol. **193:**1–24.
11. **Van Heel, M.** 1987. Similarity measures between images. Ultramicroscopy **21:**95–100.
12. **Wang, G., and M. J. Mulligan.** 1999. Comparative sequence analysis and predictions for the envelope glycoproteins of foamy viruses. J. Gen. Virol. **80:**145–154.
13. **Weissenhorn, W., A. Dessen, S. C. Harrison, J. J. Skehel, and D. C. Wiley.** 1997. Atomic structure of the ectodomain from HIV-1 gp41. Nature **387:** 426–430.
14. **Wilk, T., B. Gowen, and S. D. Fuller.** 1999. Actin associates with the nucleocapsid domain of the human immunodeficiency virus Gag polyprotein. J. Virol. **73:**1931–1940.
15. **Wyatt, R., and J. Sodroski.** 1998. The HIV-1 envelope glycoproteins: fusogens, antigens, and immunogens. Science **280:**1884–1888.
16. **Zemba, M., T. Wilk, T. Rutten, A. Wagner, R. M. Flügel, and M. Löchelt.** 1998. The carboxy-terminal $p3^{Gag}$ domain of the human foamy virus Gag precursor is required for efficient virus infectivity. Virology **247:**7–13.